Heliyon 6 (2020) e05161

Contents lists available at ScienceDirect

Heliyon

journal homepage: www.cell.com/heliyon

Research article

Anti-metastatic action of an N^4-aryl substituted thiosemicarbazone on advanced triple negative breast cancer.

A.M. Sólimo [a,b], M.C. Soraires Santacruz [c,d], S. Vanzulli [e], O. Coggiola [f], E. Bal de Kier Joffé [a,b], L. Finkielsztein [c,d], M.A. Callero [a,b,*]

[a] Universidad de Buenos Aires, Instituto de Oncología "Ángel H. Roffo", Área Investigación, Dpto. Inmunobiología, Ciudad Autónoma de Buenos Aires, Argentina
[b] Consejo Nacional de Investigaciones Científicas y Tecnológicas (CONICET), Argentina
[c] Universidad de Buenos Aires, Facultad de Farmacia y Bioquímica, Departamento de Farmacología, Cátedra de Química Medicinal, Ciudad Autónoma de Buenos Aires, Argentina
[d] CONICET-Universidad de Buenos Aires, Instituto de Química y Metabolismo del Fármaco (IQUIMEFA), Ciudad Autónoma de Buenos Aires, Argentina
[e] Instituto de Investigaciones Hematológicas (IIHEMA), Academia de Medicina, Ciudad Autónoma de Buenos Aires, Argentina
[f] Universidad de Buenos Aires, Instituto de Oncología "Ángel H. Roffo", Laboratorio Central, Buenos Aires, Argentina

ARTICLE INFO

Keywords:
Cell biology
Biochemistry
Molecular biology
Cancer research
Oncology
Triple negative breast cancer
Thiosemicarbazones
Metastasis
Invasion
Stem cells

ABSTRACT

Purpose: Advanced triple negative breast cancer (ATNBC) is defined by a lack of expression of hormones receptors as well as HER2/neu and its high probability of visceral metastasis. This pathology is associated with a poor prognosis. Previously, we found that T2, an N^4-arylsubstituted thiosemicarbazone (N^4-TSC), had cytotoxic effect on human breast cancer cells lines. Hence, in this study, we investigated the anti-metastasic action of T2 on ATNBC.

Methods: In order to deepen T2 action mode on ATNBC, we first confirmed T2 cytotoxicity on a panel of TNBC cells and then continued studying T2 effects *in vitro* an *in vivo* on the syngeneic 4T1 mouse model.

Results: We found that T2 had a cytotoxic effect comparable to chemotherapeutics used in present treatment schemes for ATNBC. T2 treatment not only induced apoptosis, but it also down-modulated 4T1 invasive and metastatic-associated capacities, such as clonogenicity, migration and metallo-proteases activity. Moreover, this agent reduced the number of 4T1 cancer stem cells. Finally, T2 treatment induced a more differentiated cell phenotype and the overexpression of the metastasis suppressor gene NDRG-1. *In vivo* assays showed that T2 reduced tumor burden, down modulated local tumor invasion and significantly reduced the number of lung metastases in the 4T1 advanced TNBC murine model, while the compound did not exhibit intolerable toxicity.

Conclusion: This study provided evidence that T2 not only exerted an anti-tumor activity but it also showed anti-invasive and anti-metastatic actions on ATNBC *in vivo* and *in vitro*, suggesting that T2 could be considered as a promising therapy that deserves further analysis.

1. Introduction

Breast cancer (BC) is the most frequently diagnosed and the second main cause of cancer-related deaths among women worldwide [1]. While a wide spectrum of treatment options is available, the therapeutic choice depends on its heterogeneous nature [2]. BC is classified into four major molecular subtypes, considering three biomarkers: Estrogen Receptor (ER), Progesterone Receptor (PR) and overexpression of human epidermal growth factor receptor 2 (HER2) [3, 4]. This classification includes the groups: (i) luminal A (ER+/PR+/HER2−); (ii) luminal B (ER+/PR+/HER2+); (iii) HER2+; and (iv) triple negative (TNBC; ER−/PR-/HER2−). Each of these subtypes has different risk factors for incidence, therapeutic response, disease progression, and different organ sites of metastases. Most BC patients (83%) have tumors with hormone receptors expression, BC patients that are HER2+ constitute only 5% and TNBC includes the remaining 12% of the total patient population [5].

Advanced triple negative breast cancer is the most aggressive and difficult subtype to treat. The principal treatment is standard chemotherapy, usually consisting of taxanes, anthracycline, and platinum drugs [6, 7]. Several targeted therapies such as Epidermal Growth Factor Receptor (EGFR) inhibitors, antiangiogenic agents, DNA repair agents, checkpoint kinase 1 inhibitors or poly-ADP-ribose-polymerase (PARP)

* Corresponding author.
E-mail address: mcallero33@gmail.com (M.A. Callero).

https://doi.org/10.1016/j.heliyon.2020.e05161
Received 28 July 2020; Received in revised form 8 September 2020; Accepted 1 October 2020

inhibitors have been tested for metastatic TNBC treatment; however, no substantial improvements in TNBC outcomes have been observed with these agents [8].

Although, ATNBC is the BC subtype with the most complete response to chemotherapy (22%), recurrence and metastasis rates for these patients are higher than for those carrying other BC subtypes [9]. Due to the lack of receptors expression, the use of targeted therapies in high grade TNBC tumors is precluded, leaving chemotherapy as the only approved systemic treatment option. Considering the suboptimal treatment results with current chemotherapy, new therapies for TNBC are critically required.

Thiosemicarbazones (TSCs) are iron chelators obtained from a condensation reaction between a thiosemicarbazide with an aldehyde or ketone. Among their biologic activities, the anti-tumoral effect has been recently investigated [10, 11, 12, 13]. The molecular mechanisms involved in the activity of TSCs have not been completely understood, however, several modes of action have been reported.

Previously, we reported that two of three studied N^4-aryl substituted thiosemicarbazones (N^4-TSC) had cytotoxic effect on a group of different human breast cancer cell lines. Cell death by apoptosis and necrosis via ROS formation and ribonucleotide reductase inhibition were the events observed in response to these N^4-TSCs treatment [14].

Taking into consideration the need for ATNBC therapies, in this study, we explored the action of T2, the most potent N^4-TSCs previously studied and characterized [14], on metastasis and tumor dissemination *in vitro* and *in vivo* in the 4T1 triple negative mouse mammary model that resembles advanced breast cancer [15, 16]. Our results demonstrate that T2 not only suppressed ATNBC cell growth and induced apoptosis, but it also down-modulated 4T1 metastasis-associated properties and diminished cancer stem cell sub-population *in vitro*. In addition, *in vivo* studies demonstrated that this N^4-TSC also reduced tumor burden as well as its local invasiveness and metastatic capacity. These findings describe a novel activity for T2 and propose this compound as a promising anti-tumoral and anti-metastasic agent against late-stage TNBC, thus supporting further investigation.

2. Methods

2.1. In vitro studies

2.1.1. Cell lines

The 4T1 murine mammary cancer cell line was obtained from ATCC and cultured in RPMI medium supplemented with 10% fetal bovine serum. LM38-LP cells were isolated from a mammary papillary triple negative adenocarcinoma that developed spontaneously in a Balb/c mouse [17]. These cells were grown in DMEM-F12 medium supplemented with 10% fetal bovine serum (FBS) and 80 μg/ml gentamycin.

The HCC70 human breast cancer cell line, derived from a primary ductal triple negative carcinoma and obtained from ATCC, was cultured in RPMI medium supplemented with 10% FBS. All cell lines were cultured in 25 cm2 flasks at 37 °C in a humidified air atmosphere with 5% CO2.

Cells lines were tested for mycoplasma contamination by DAPI stain monthly and by PCR every 3 months.

2.1.2. Cytotoxicity assay

Cells grown in 25 cm^2 flasks were removed by trypsinization and seeded into 96-well culture dishes at a concentration of 1,000 cells per well. Cells were allowed to grow for 48 h at 37 °C in a humidified atmosphere containing 5% CO_2. Then cells were treated with T2 at the following concentrations: 0.1, 1, 10, 25, and 50 μM or with DMSO (0.1%) (control) for additional 120 h 4T1 cells were also treated with Cisplatin or Paclitaxel with the same concentration as T2. Cell viability was determined by the MTS method [18]. The IC_{50} were determined through non-linear regression analysis using the concentration log-response curve for each cell line employing PrismGraph software.

2.1.3. Colony formation assay

4T1 cells treated with T2 (2.5, 5 or 10 μM) or DMSO 0.02% (control) for 24 h, were harvested with trypsin-EDTA and counted manually in the presence of Trypan blue. Then, cells were diluted and seeded at about 1,000 viable cells per well of a six-well plate. After incubation for 7–10 days, cells were washed twice with PBS, fixed with methanol:acetic acid for 15 min, and stained with 0.5% crystal violet for 15 min at room temperature. A colony was defined to consist of at least 20 cells. Colonies were counted under a stereoscopic microscope. Clonogenic capacity was calculated with the following formula:

$$\text{Clonogenic Capacity} = \text{number of colonies} / \text{number of seeded cells}$$

2.1.4. Quantification of apoptosis

Apoptotic/necrotic cells were determined by Annexin V-FITC and propidium iodide staining. To do so, cells were seeded in six-well plates, treated with T2 (2.5, 5 or 10 μM) or DMSO 0.02% (control) for 48 h, and washed. Then, cells were removed by trypsinization and stained. Fluorescence was measured by flow cytometry and analyzed using Cyflogic software version 1.2.1.

Western blot analyses using antibodies against caspase 3 (Cell Signaling #9662S 1:1000), poly(ADP-ribose) polymerase (PARP) (Cell Signalling #9532S, 1:1000) and Bcl-XL (Abcam #ab322370, 1:1000) were performed using total lysates of 4T1 cells treated with T2 or DMSO as previously described. Actin was used as loading control.

2.1.5. Wound healing assay

4T1 cells were seeded in six-well plates and incubated for 48 h to achieve an 80–90% confluent monolayer. Cells were treated for 24 h with 2.5, 5 or 10 μM T2. After this time had elapsed, a single scratch wound was created in the monolayer with a yellow tip. The wound was photographed under a phase contrast microscope at time 0 and approximately 17 h later (final time, Tf). Cell migration was assessed by determining the covered area at T_0 and T_f in four fields per well with ImageJ software; then the percentage of migration was calculated using the following equation:

$$(Tf - T0) / T0$$

2.1.6. Gelatin zymography assay

Activity of metaloproteinases (MMPs) was analyzed by a gelatin zymography assay as previously described [19]. Cells were seeded in 6-well plates and grown for 48 h in medium containing 10 % FBS. Then, cells were treated with DMSO or T2 (2.5, 5 or 10 μM) for 24 h. The cell conditioned media were electrophoresed in a 10 % polyacrylamide gel containing 0.1 % gelatin. After electrophoresis, the gel was incubated at 37 °C overnight in a buffer (50 mM Tris, pH 8.0, 10 mM $CaCl_2$ and 1 mM $ZnCl_2$) to facilitate gelatin degradation by gelatinase. The gel was washed with water and subsequently stained with 0.5 % Coomassie brilliant blue R250 and destained in destaining solution (methanol:acetic acid:water in the ratio of 4:1:5). Gelatinase activity was measured densitometrically after scanning the gel. Bands were quantified in arbitrary units using Image J and relativized to total protein content.

2.1.7. Transwell invasion assay

4T1 cells treated with T2 (2.5, 5 or 10 μM) or DMSO (control) for 24 h were seeded on transwell chambers (8 microns' pore size) coated with Matrigel [20]. Then cells were stimulated by filling bottom reservoir with medium containing 10% FBS for 5 h. Membranes were fixed, stained with DAPI, observed under fluorescence microscope and then imaged to quantify the number of cells that migrated to the bottom side of the membrane.

2.1.8. Mammosphere formation assay

4T1 cells treated with T2 (2.5, 5 or 10 μM) or DMSO 0.02% (control) for 24 h were trypsinized and grown in suspension in six-

well low attachment culture plates at a density of 5,000 viable cells/ml in the presence of serum-free media supplemented with B27 and EGF. Resulting mammospheres were manually counted after 5–8 days in culture using a Nikon eclipse TE2000-S phase contrast inverted microscope. Mammospheres were also imaged and photographed under the same microscope. Diameters were measured with Image J software. Fifteen to twenty fields per plate were used to calculate diameter average of mammospheres.

2.1.9. In vitro treatment of mammospheres

4T1 cell were used to generate mammospheres as previously described. After 5–8 days, mammospheres were exposed to T2 T2 (2.5, 5 or 10 μM) or DMSO (control) for 24 h and visualized under Nikon eclipse TE2000-S phase contrast inverted microscope.

2.1.10. Flow cytometry analyses for cancer stem cell sub-population

Treated 4T1 cells were harvested and resuspended in PBS following staining to detect CD24-APC, CD29-FITC and LIN-PE employing the PASIII (PARTEC) cytometer. Population analysis was made using FlowJo software.

2.1.11. Evaluation of pluripotent genes expression

Total RNA from 4T1 cells treated with T2 (2.5, 5 or 10 μM) or DMSO 0.02% (control) for 24 h was isolated using Trizol Reagent. RNA concentration was estimated by measuring the optical density at 260 nm and 2 μg RNA was reversely transcribed by using M-MLV Transcriptase (1U) and random hexamers (50 ng/μl). Real-Time PCR for Nanog, Oct-4 and Sox-2 was performed in a 20 μl master mixture of TransStar Green Kit and specific primers were used at 0.25 μM. Real-Time PCR reactions were performed in a C1000 Thermal Cycler (Biorad) and the amplification program consisted of an initial denaturing step (94 °C for 5 min), followed by 40 cycles (each of 94 °C for 30 s, 60 °C for 30 s and 72 °C for 30 s). Sample quantification was normalized to endogenous GAPDH that was also quantified by Real-Time PCR, following the same protocol as that for pluripotent genes. Fluorescence signal acquisition was carried out at the end of the elongation step. Each assay included a DNA minus control. All samples were run in duplicate and the experiment repeated 3x with independently isolated RNA. RNA expression changes were calculated using the $2^{-\Delta\Delta Ct}$ method.

2.1.12. Evaluation of NDRG-1 and E-cadherin expression

4T1 cells were treated with T2 (2.5, 5 or 10 μM) or DMSO 0.02% (control) for 24 h. Total RNA extraction and reverse transcription were performed as previously described. Real time PCR for NDRG-1 was carried out using specific primers and the amplification program consisted of an initial denaturing step (94 °C for 5 min), followed by 40 cycles (each of 94 °C for 30 s, 56 °C for 30 s and 72 °C for 30 s). Sample quantification was normalized to endogenous GAPDH which was also quantified by Real-Time PCR [21], following the same protocol as that for NDRG-1. Fluorescence signal acquisition was carried out at the end of the elongation step. Each assay included a DNA minus control. All samples were run in duplicate and the experiment repeated 3x with independently isolated RNA. RNA expression changes were calculated using the $2^{-\Delta\Delta Ct}$ method.

For protein expression, confluent monolayers of 4T1 cells previously treated with T2 (2.5, 5 or 10 μM) or DMSO 0.02% (control) for 24 h were washed three times with ice cold PBS and then lysed with Lysis Buffer (RIPA with EDTA) containing protease inhibitors cocktail. Protein content of cell samples was determined by Bradford method [22]. The samples were boiled in Laemmli sample buffer with 5% β-mercaptoethanol. Western Blot analyses were carried out using SDS-PAGE. Electrophoresis gels were transferred to PVDF membranes. Non-specific binding was blocked by incubation of the membrane with TBS 5% skim milk for an hour. Then, membranes were incubated with the specific antibodies against NDRG-1 (Santa Cruz, sc-398291, 1:1000) or E-cadherin (Abcam, #ab76055, 1:1000) overnight at 4 °C.

2.1.13. Immunofluorescence

Cells were grown on glass coverslips and treated with T2 (2.5, 5 or 10 μM) or DMSO 0.02% (control). After 24 h, cells were fixed in 4% formaldehyde/PBS at room temperature for 15 min, permeabilized and blocked with PBS 5% SFB + 0.3% triton for 90 min at 37 °C. Smooth muscle actin (SMA) was detected by incubation with a primary monoclonal antibody (Sigma #120M468, 1:500), followed by incubation with an anti-mouse IgG-Alexa 488 secondary antibody (1:500) for 1 h (Invitrogen-Thermo Fisher Scientific). Nuclei were stained with propidium iodide. Images were obtained in an Olympus Fluo view FV 1000 microscope. The quantitative microscopy measurements were performed in individual cells (13–745 cells for each treatment or condition). Confocal microscope images were processed with FIJI (https://fiji.sc). Channel backgrounds (mean of empty region) were substracted. Segmentation of the nuclear compartment was performed for each cell using the IP signal.

For F-Actin staining, coverslips were incubated for 45 min at RT with phalloidin-FITC (Sigma-Aldrich, 1:400) and cell nuclei were counterstained with DAPI. The coverslips were mounted with Mowiol 4–88 (Calbiochem). Cells were imaged by confocal laser scanning microscopy, which was performed with the same microscope but using an Olympus 60×/1.20 NA UPLA APO water immersion objective and a 3x digital zoom. Graphic depiction was then generated where the x-axis represented the distance across the cell and the y-axis represented the level of fluorescence. Twelve cells were randomly selected from each group of treatment for graphic depicting.

2.2. In vivo studies

2.2.1. Animals

Inbred 3–4 month old BALB/c female mice (20–25 g body weight) were obtained from the Animal Care Division of the Research Area of the Institute of Oncology "Angel H. Roffo". All applicable international, national, and/or institutional guidelines for the care and use of animals were followed. Specific protocols used in this study were approved by the Ángel H. Roffo Institute IACUC (approved protocol number 2017/01).

2.2.2. Determination of the maximum tolerated dose (MTD) in control healthy BALB/c mice

The starting dose of T2 was determined by a review of the literature in which other thiosemicarbazones were used [10, 23]. The MTD was defined as the dose level at which 30% or less of a cohort either died or lost weight in excess of 10%. Cohorts of 5–10 BALB/c mice were used in toxicity experiments and received T2 (5, 25 or 50 mg/kg) or equal volumes of 0.9% NaCl solution or vehicle (saline solution with 17% DMSO and 30% propilenglycol) to determine the MTD. Treatments were given i.p., 5 times every two days. Mice were monitored daily and weighted every 3 days. After necropsy, blood samples were collected and serum concentrations of urea and glutamic oxaloacetic transaminase (GOT or AST) were determined. The blood samples were also used to determine erythrocyte and leukocyte counts, hemoglobin and hematocrit. The hematological analyses were performed in the clinical analysis laboratory of our institute. The values obtained were compared within and between groups. At the end of the experimental period (30 days) histopathological analyses of the lungs, liver and kidneys were performed.

2.2.3. Tumor growth and spontaneous metastases capacity

4T1 cells ($3{,}5 \times 10^4$) were injected subcutaneously and after one week T2 treatment was initiated. For animal dosing, T2 was prepared as a smooth suspension in saline solution containing 17% DMSO and 30% propilenglycol. Each experiment ($n = 18$ mice) contained a vehicle control group treated in parallel with the T2-treated groups. T2 was evaluated at two dose levels ($n = 6$ mice per dose) given intraperitoneally. The treatment schedule comprised 5 doses once a day administered day through. After 25–30 days, animals were euthanatized, and tumors were weighed and then fixed in formaldehyde. Lungs were removed and fixed with Bouin's solution. Spontaneous metastatic nodules were

counted under a stereoscopic microscope. The experiment was performed three times.

2.2.4. Experimental metastases

4T1 cell monolayers treated with T2 (2.5, 5 or 10 μM) or DMSO 0.02% (control) for 24 h were trypsinized, resuspended in serum free RPMI and injected into the tail vein of BALB/c mice at 4×10^4 cells/100 μl. After three weeks, mice were sacrificed, and lungs were fixed in Bouin's solution. Superficial metastatic nodules were observed, imaged and counted under stereoscopic microscope.

2.2.5. Histopathological analysis

For the histopathological analysis, lungs, liver, kidneys and tumors were collected and fixed by immersion in a 10% buffered formaldehyde solution for 24h, followed by dehydration in increasing concentrations of alcohol, incubation in xylol and soaking in paraffin. The sections were cut to 5 μm thickness and stained with hematoxylin and eosin (HE) or Masson's Trichrome for histopathological analysis. Mitotic figures were counted under microscope (Magnification 400 x). Histopathologic analysis was done by external accredited experimental pathologists.

2.2.6. Statistical analyses

Differences between groups were analyzed using one-way ANOVA with Tukey's test or the Tukey–Kramer multiple comparison test for evaluating three or more groups. For in vivo assays, statistical significance was determined using non-parametrical analyses with comparisons by Kruskal–Wallis, Dunn's post test. Statistical analysis was performed using GraphPad Prism 4.0, Graph Pad software, Inc. San Diego, California, USA, www.graphpad.com. Differences were considered significant at $p < 0.05$.

3. Results

3.1. T2 induces 4T1 cell death by apoptosis

Considering the need to find new therapies for metastasic advanced TNBC, we decided to deepen the study of the action of T2 on this breast cancer subtype. Therefore, we first confirmed its effects *in vitro* on a triple negative breast cancer cells panel composed by the murine 4T1 and LM38-LP cell lines and the human HCC70 cell line.

As Figure 1B shows, when we compared cell viability in TNBC cell lines after T2 treatment in a dose range between 0 and 50 μM, we observed a potent cell growth inhibition on all cell lines. The concentration of T2 required to reach 50% of control untreated cells was 5.9 μM, 3.16 μM and 3.40 μM for 4T1, LM38-LP and HCC70 cells, respectively. Besides, after treating 4T1 cells with Cisplatin or Paclitaxel, we found comparable IC_{50} values for these two current treatments for TNBC (6.21 μM and 6.32 μM, respectively, data not shown). Considering 4T1 as a representative advanced triple negative model, and taking into account the certain possibility of developing *in vivo* assays in syngeneic mice, we decided to continue our experiments with this cell line using the established T2 concentrations of 2.5, 5 y 10 μM.

Flow cytometry analysis of cells treated with T2 for 48 h and stained with Annexin V and propidium iodide revealed that T2 lowest concentration used was enough to cause a significant increase in the number of both early and late apoptotic cells compared to control cells treated with

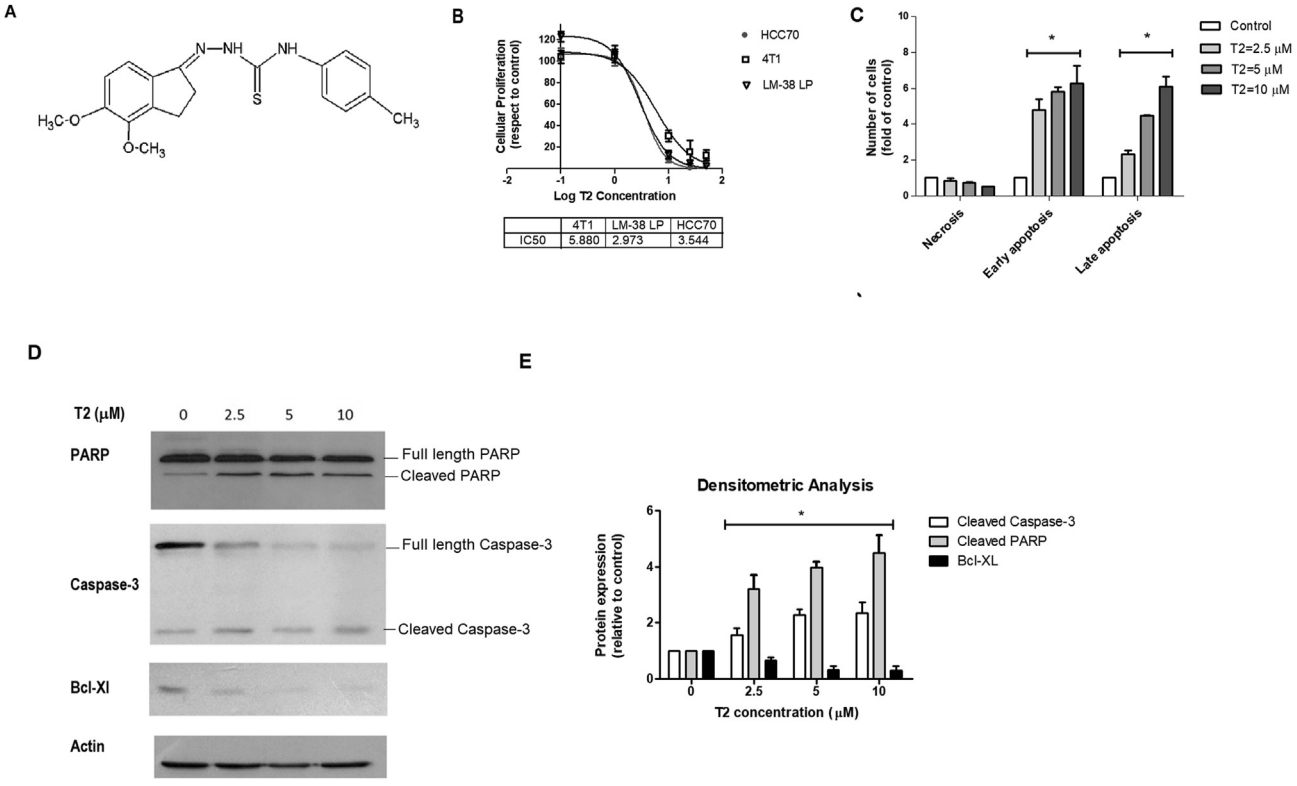

Figure 1. T2 reduces cell viability in triple negative breast cancer cell lines and induces apoptosis. (A) T2 formula. (B) Concentration log-response curve: results from MTS viability assays examining the effects of T2 on the growth of 4T1, LM38-LP and HCC70 cell lines. Cells were incubated with T2 or DMSO (control) for 5 days. (C) Cell apoptosis determined by Annexin V-FITC and propidium iodide staining. Flow cytometer analysis of the apoptotic and necrotic cells after 24 h of incubation with T2 (2.5, 5 and 10 μM) or DMSO (control). Results are expressed as mean ± standard deviation, *$p < 0.05$ (n = 3). (D) Western blots illustrating PARP cleavage, caspase-3 activation and Bcl-xL induction after T2 (2.5, 5 and 10 μM) or DMSO (control) treatment for 24 h. A representative blot of three is shown. (E) Densitometric analyses of three independent western blots.

the vehicle DMSO, suggesting that T2 activates some pathway leading 4T1 cells to death by apoptosis (Figure 1C).

To further investigate T2 effect on 4T1 cells death, we carried out Western Blot experiments upon separated proteins of whole cell lysates following treatment with T2 during 48 h. As seen in figures 1D and E, treatment with T2 induced caspase-3 activation, observed as an increase in proteolytic processing of its inactive zymogen into the activated p17 fragment. In accordance with this result, PARP cleavage, and Bcl-XL expression downregulation were observed after T2 treatment. Full, non-adjusted images are shown in supplementary material.

3.2. T2 reduces the clonogenicity, migration and invasiveness of 4T1 cells

Previously we have observed that T2 reduced clonogenicity and migration in MDA-MB231 cells [14]. In order to analyze whether T2 exerted similar actions on 4T1 cells, the anticancer activity of T2 was further studied using a short 24h-treatment, an experimental condition that did not show cell cytotoxicity. First, we performed a clonogenic assay. As shown in Figure 2A, T2 treatment during 24 h induced a significant inhibition of colony formation starting at the concentration of 2.5 μM and showing a dose-dependent modulation.

Since tumor cell migration and invasiveness are key determinants in tumor progression and metastatic dissemination, we tested whether T2 modulates the migration ability of 4T1 cells by performing a wound-healing assay. We observed a significant decrease in the cells capacity to close the wound with the three assayed concentrations of T2 (Figures 2B and C).

Considering that matrix metalloproteases are enzymes with a relevant role in cell invasion, we studied the activity of the matrix metalloprotease 2 and 9 (MMP2 and MMP9, respectively) through zymograms (Figure 2D) and found that MMP9 activity was significantly reduced after treating 4T1 cells with 10 μM T2 for 24 h while MMP2 activity was not modulated by T2. Full, non-adjusted images are shown in supplementary material. Taking into account that one of the factors relevant for the invasive process was altered by T2 treatment, we went on to further study this aspect using transwell chambers coated with Matrigel and FBS in the lower compartment used as chemoattractant. T2 treatments significantly reduced the invasive capacity of 4T1 cells to reach the filters after degrading the Matrigel (Figure 2E).

3.3. T2 diminishes cancer stem cells (CSC) sub-population of 4T1 cell line

In order to determine whether T2 could affect 4T1 CSCs, we performed a mammosphere forming assay using 4T1 cells previously treated with T2 for 24 h. As shown in Figure 3A, 5 and 10 μM T2 caused an evident reduction in mammosphere number (left) and a significant decrease in mammosphere size (right). Consistent with these results, we observed a decrease in the percentage of 4T1 cells that expressed high concentration of CD29, a CSC marker (Figure 3B.) In addition, we found a lower expression of the pluripotency associated genes Nanog, Oct-4 and Sox-2 in T2 treated cells, compared with untreated control cells (Figure 3C). Since a 24h treatment with T2 did not induce cytotoxicity, downregulation of these genes expression could be associated with a smaller population of stem cells.

We then sought to determine T2 action on already formed mammospheres. Treatment with T2 showed a direct cytotoxic effect, observed by a spheres disruption. Mammospheres were dissociated and reduced in number at concentrations of 5 and 10 μM of T2 (Supp. Figure 1), suggesting CSCs cell death induced by T2.

3.4. T2 decreases experimental metastatic capacity of 4T1 cells

In the metastatic process, upon cells detachment from the tumor, their capacity to survive in the blood stream and colonize other tissues is crucial. In order to assess this key aspect, we performed an experimental metastasis assay. Cells were pre-treated *ex-vivo* with T2 for 24 h and then inoculated intravenously in BALB/c mice. Three weeks later, mice were euthanized and the number and size of superficial metastatic nodules in their lungs were recorded We found that the total number of metastatic nodules was significantly reduced when cells were pre-treated with 5 and 10 μM T2 (Figure 4). . Similarly, when nodules were distributed by size, 5 and 10 μM T2 showed a significant reduction of metastatic nodules larger than 0.5 mm diameter (Supplementary Figure 2).

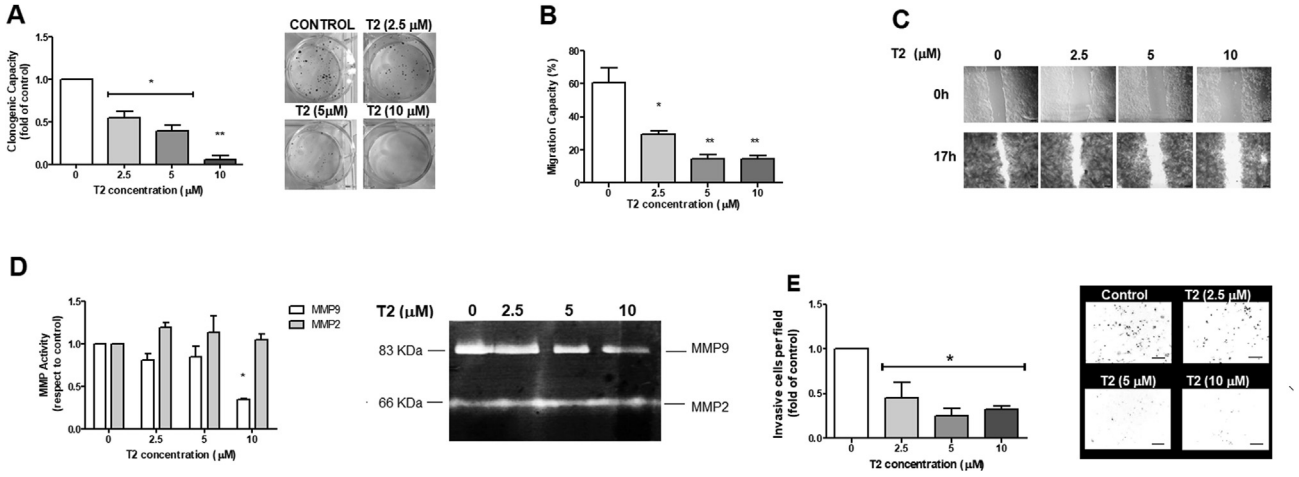

Figure 2. T2 downmodulates metastasis-related properties of 4T1 cells (A) Clonogenic assay was done with 4T1 cells pre-incubated with T2 (2.5, 5 and 10 μM) or DMSO (control) for 24 h. The values represent the mean of three independent experiments, *$p < 0.05$ or **$p < 0.01$ with respect to control cells. (B) Migration assay: 4T1 cells were treated with T2 (2.5, 5 and 10 μM) or DMSO (control) for 12 h. The graph shows the migration percentage for each T2 treatment. Values that are significantly different from controls are indicated *$p < 0.05$ or **$p < 0.01$, (magnification 200×, scale bar 40 μm) Experiments were performed in triplicate. (C) Representative fields from one migration experiment are shown. (D) Zymogram assay was used to evaluate MMP9 gelatinase activity: 4T1 cells were treated with T2 (2.5, 5 and 10 μM) or DMSO (control) for 12 h and conditioned media were run. Upper panel: Representative gelatin zymography gel. Lower panel: densitometric analyses of MMP-9 activity. Data represent the relation between the optical density and total protein concentration. The values represent the mean of three independent experiments, **$p < 0.01$ respect to control cells. (E) Invasion capacity was analyzed by a Transwell chamber assay. Cells were treated as previously described. Left panel: Results are expressed as mean ± standard deviation ($n = 3$). Right panel: representative micrographs from one of three independent experiments (Magnification ×100, scale bar 40 μm).

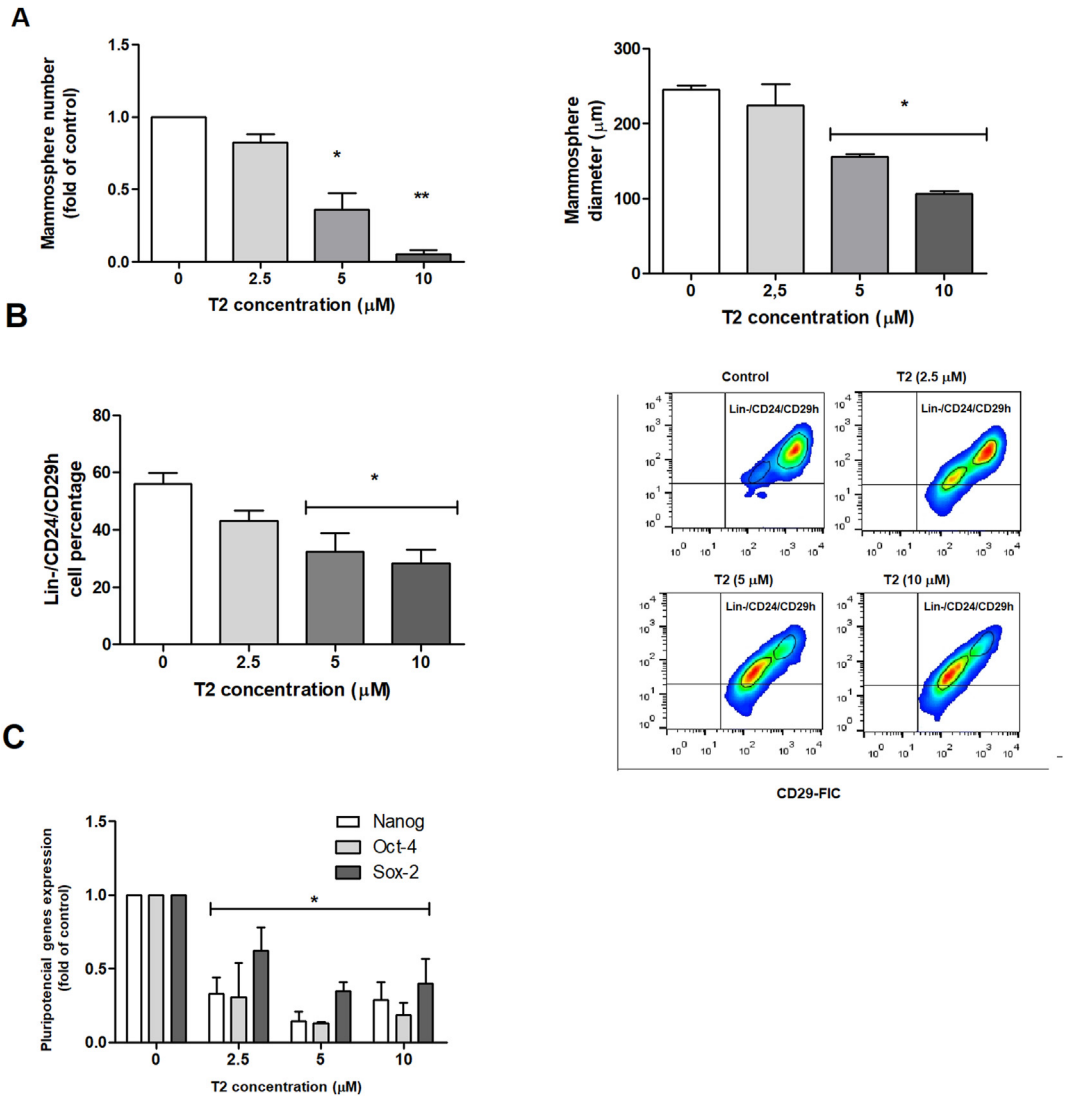

Figure 3. T2 reduces CSC subpopulation in 4T1 cells. Cells were treated with T2 or DMSO (control) for 48 h. (A) Mammospheres number and size (diameter) were evaluated after a 5–8 days culture in mammosphere formation conditions. Data represent the mean of at least three independent experiments, *$p < 0.05$ or **$p < 0.01$ with respect to control cells. (B) Flow cytometry for Lin(-)/CD29h/CD24(+) expression in 4T1 cells. Data are the mean of at least three independent experiments. *$p < 0.05$ or **$p < 0.01$ compared to control untreated cells. (C) Expression of pluripotential genes analyzed by real time PCR. Results are expressed as mean ± standard deviation ($n = 3$), *$p < 0.05$ with respect to control cells.

3.5. T2 induces NDRG-1 expression on a post-traductional level

It has been reported that human NDRG-1 (N-myc down regulated gene), could act as a metastasis suppressor in several types of cancer [24, 25]. In addition, NDRG-1 expression was reported to be up-regulated by other thiosemicarbazones such as Dp44mT and DpC [23]. Moreover, breast cancer metastasis was reported to be inhibited by Dp44mT *in vivo*, which effect was dependent on its ability to up-regulate NDRG-1 [26]. Therefore, we evaluated NDRG-1 expression at mRNA and protein levels. As Figure 5A shows, we found that while T2 did not alter NDRG1 mRNA expression, it induced an increase in the amount of protein. Full, non-adjusted images are shown in supplementary material.

3.6. T2 induces a less undifferentiated phenotype in 4T1 cells

In cancer, poor cell differentiation is usually related with a worse prognosis. While the most differentiated epithelial cells show less invasive capacity and a higher expression level of adherence proteins such as E-cadherin, the undifferentiated fibroblastoid-like cells are commonly invasive and express lower levels of these proteins.

T2 treatment up-regulated E-cadherin while the expression of the myofibroblastic marker alpha smooth muscle actin (SMA) was reduced as shown both by western blot and confocal microscopy (Figure 5B and 5C, respectively). Moreover, a cortical reorganization of actin distribution was observed after staining the actin filaments of cells treated with T2 for 24 h with phalloidin-FITC (Figure 5D) evidencing a more differentiated epithelial phenotype.

3.7. T2 has anti-tumor and anti-metastatic action in vivo

To further characterize the efficacy of T2 against triple negative breast cancer and its potential as a promising anti-tumor agent, further studies examining this agent were performed *in vivo*.

In order to choose the appropriate doses to perform the antitumor studies in mice, we first evaluated the maximum tolerated dose of T2 and its acute toxicity as described in materials and methods (2.2). The highest concentration of T2 (50 mg/kg) caused death to 1/3 of the animals, so it

A

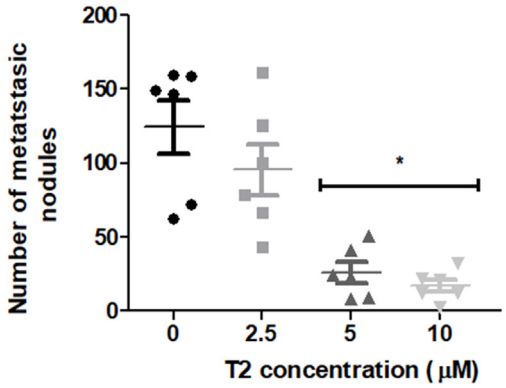

T2 Concentration (μM)	0	2,5	5	10
Median	147,5	89,00	23,50	16,50
Range	62-159	43-161	8-51	3-32

B

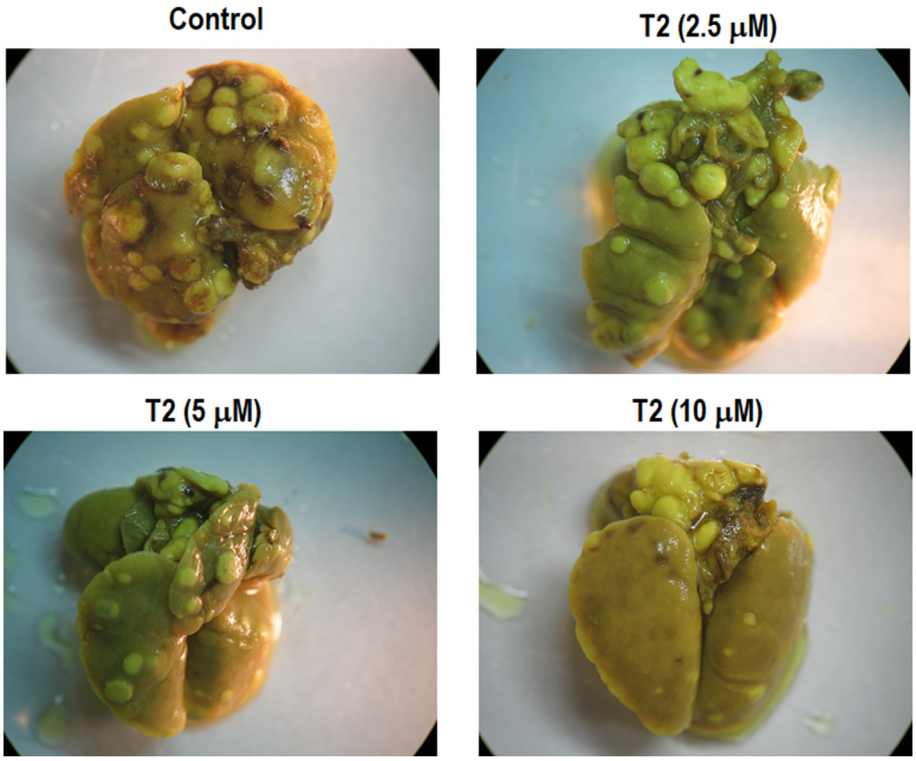

Figure 4. T2 downmodulates the experimental metatastic ability of 4T1 cells. 4T1 cells treated in vitro with T2 or DMSO (control) for 48 were injected intravenously in BALB/c mice and the number of total experimental lung metastases was recorded after 21 days. (A) Data represent metastatic nodules median and range of one representative experiment of three independent assays. *$p < 0.05$ respect to control cells. (B) Representative photograph of lung metastatic *foci*.

was discarded. Treatments with 5 or 25 mg/kg T2 were well tolerated and showed no severe clinical side effects with no mortality. Furthermore, changes either in behavior or body weight of the animals throughout the experiment were absent (Supplementary Figure 3A).

The observed hematological parameters of animals treated with T2 were within the reference limits and full hematological analysis showed no difference respect to vehicle treated mice (Data not shown). Biochemical analysis of blood taken from animals treated with T2 did not show any alteration either in urea concentration or in the enzyme glutamic oxaloacetic transaminase (AST-TGO), indicating the absence of renal and hepatic alterations in the animals of this group (Supplementary Figure 3B and 3C, respectively). Histopathological studies on the liver, heart, kidneys and lungs were performed to determine the presence of pathological alterations caused by T2. The results indicate that there was no alteration in the organs from the treated groups compared with the control.

Therefore, in order to evaluate T2 action *in vivo*, treatment consisted of five doses of vehicle or T2 (5/25 mg/kg) administered intraperitoneally every other day. Tumor weight, measured after necropsy, showed that tumors of control untreated mice reached a weight of 522,6 ± 100

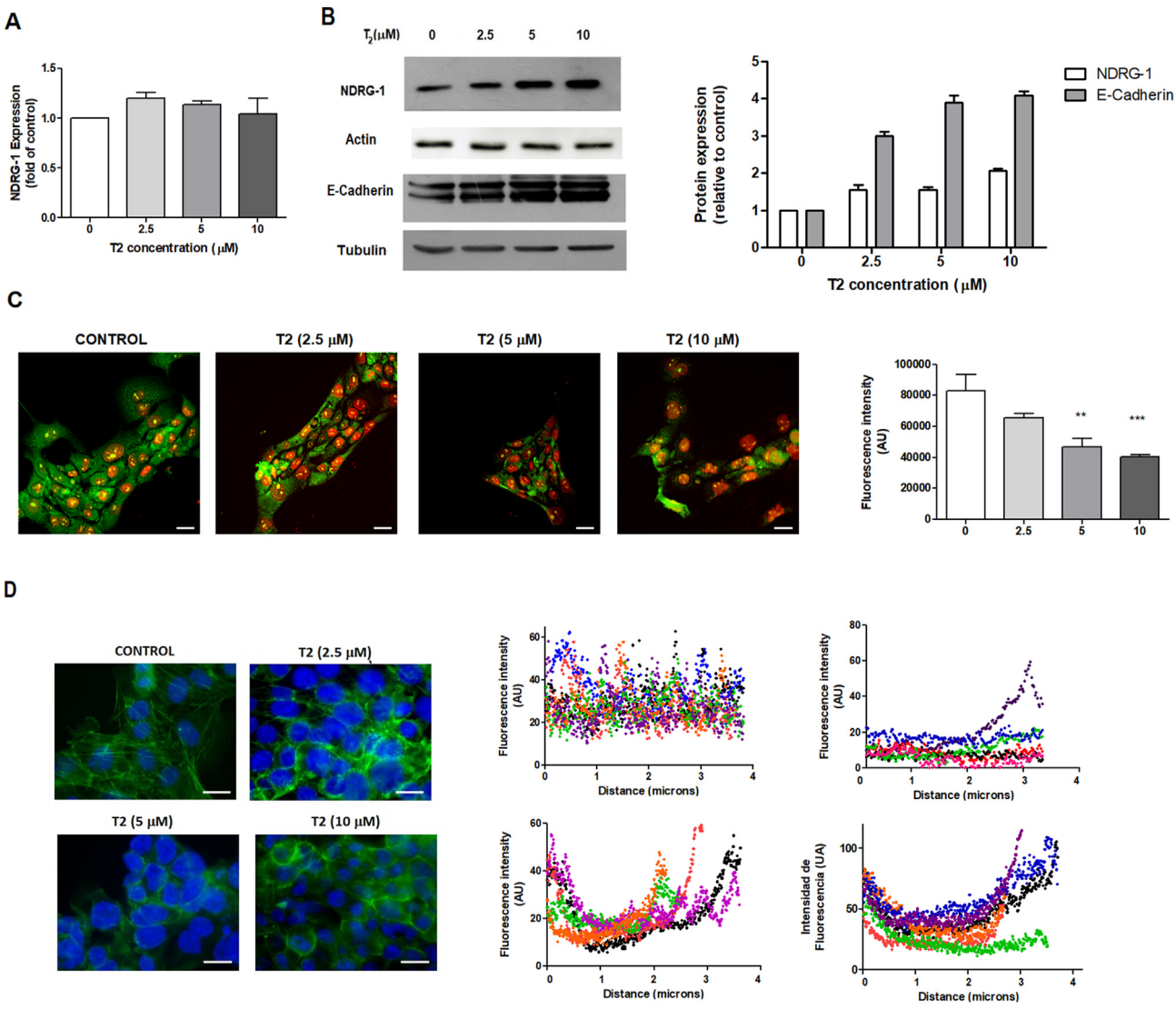

Figure 5. T2 induces NDRG-1 protein expression and a more differentiated phenotype in 4T1 cells. (A) RNA from T2 treated or control untreated 4T1 cells was isolated. The expression of NDRG-1 was evaluated by Real Time PCR. Data represent the media and standard error of three independent experiments. (B) Lysates from T2 or DMSO treated 4T1 cells were prepared, and their total protein content was subjected to SDS-Page and Western blot. Representative NDRG-1 and E-cadherin blots are shown. Tubulin was used as loading control. (C) Immunofluorescence micrograph of αSMA expression (Magnification 600×, scale bar 10 μm) and fluorescence intensity quantification of T2 or DMSO treated 4T1 cells. Nuclei were stained with propidium iodide. Data represent median and range of three independent experiments. *$p < 0.05$ respect to control cells (D) Fluorescence microscope analysis of actin cytoskeleton after phalloidin-FITC staining of T2 or DMSO treated 4 T1 cells Nuclei were stained with DAPI. Representative images are shown (Magnification x1000, scale bar 10 μm). The scatter plots represent the quantification of fluorescence intensity across the lines of 10 cells of each group using ImageJ software.

mg while T2 treatment (5 and 25 mg/kg) significantly decreased tumor weight (Figure 6A). In accordance, the average number of mitotic figures in tumors of T2 treated mice was lower than in control ones (Figure 6B).

The 4T1 tumor is a mammary adenocarcinoma with an aggressive fast-growing behavior which develops metastatic disease spontaneously from the primary tumor like triple negative BC in humans does. Moreover, the progressive spread of 4T1 metastases to the draining lymph nodes and other organs resemble that of human BC. Interestingly, after necropsy, we found that although 63 ± 3% of control tumors were able to invade the abdominal muscle wall and parietal peritoneum, and then colonize the peritoneal cavity of mice, only 40.0 ± 1.0% and 22.5 ± 2.5% of T2-treated ones (5 and 25 mg/kg, respectively) had this ability (Figure 6C). Moreover, microscopic examination of the tumor revealed infiltrative edges in control mice tumors with disruption of collagen fibers distribution (pointed with an arrow). However, in T2 treated mice tumors, there was less evidence of invasion with less expansive edges and collagen fibers appeared more straight and aligned parallel to the tumor border (Figure 6D). With respect to blood dissemination, the T2 treated mice developed a significantly lower number of spontaneous lung metastases per mouse compared with control untreated mice (Figure 6F).

4. Discussion

Advanced triple negative cancer is considered as one of the most frequent causes of cancer-related mortality in women worldwide [1]. Moreover, it is the most aggressive and challenging to treat among breast cancers. Although TNBC shows the most complete response to chemotherapy, among different breast cancer subtypes, patients with late-stage TNBC tumors have a less satisfactory prognosis than those with other breast cancer tumors. In addition, most patients with advanced TNBC succumb to metastasis. Increasing researches suggest that iron chelators can be used as new anti-cancer drugs accomplishing critical impact in different cancers treatment [27, 28, 29]. In this context, we have previously demonstrated that two N^4-aryl substituted thiosemicarbazones had

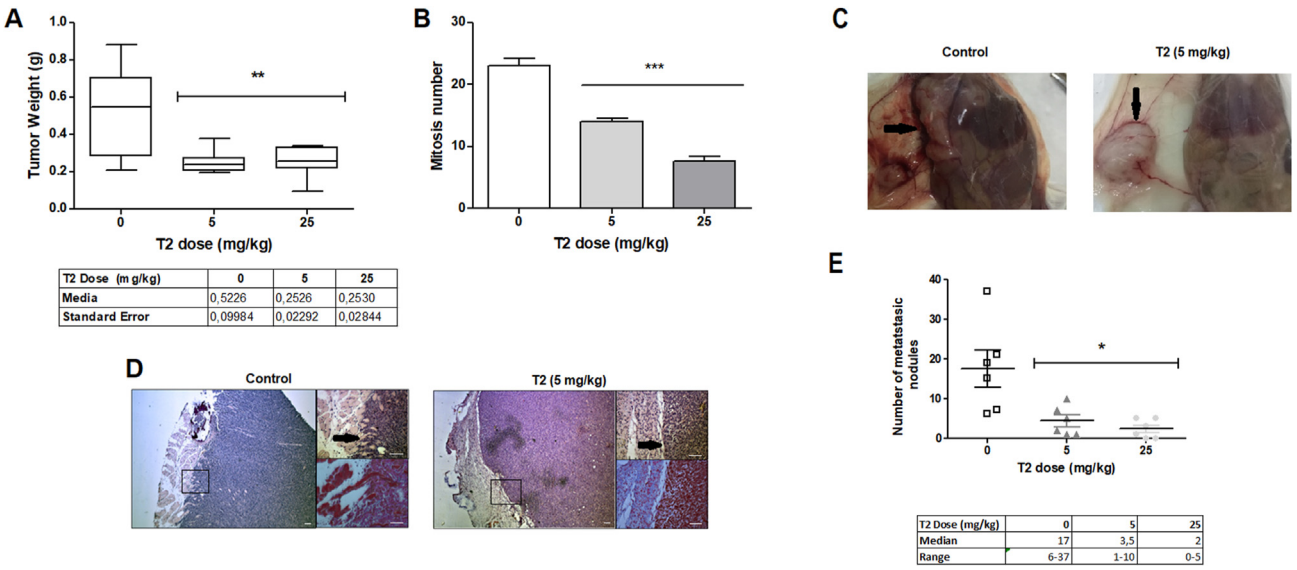

T2 Dose (m g/kg)	0	5	25
Media	0,5226	0,2526	0,2530
Standard Error	0,09984	0,02292	0,02844

T2 Dose (mg/kg)	0	5	25
Median	17	3,5	2
Range	6-37	1-10	0-5

Figure 6. In vivo treatment with T2 inhibited 4T1 tumor growth, invasion and metastasis. 3.5 x 10^4 4T1 cells were injected subcutaneously into female BALB/C mice. After one week mice were injected intraperitoneally with vehicle (control) or T2 (5 or 25 mg/kg of body weight) 5 times every two days (n = 6 mice per group) as described in materials and methods. (A) Tumor weight after necropsy. Plot of a representative experiment of three independent assays, *p < 0.05 respect to control cells. (B) Number of mitotic figures per ten analyzed fields, counted under microscope from hematoxylin-eosin stained tumor sections. Data represent the media and the standard error of three independent experiments, ***p < 0.001 respect to control cells. (C) Illustrative examples of differential peritoneal invasion and (D) hematoxylin-eosin (H&E) and Masson's Trichromic staining of tumors are shown. Arrow points tumor edge (Magnifications 100× (left pannel) and 200× (right panel), scale bar 200μm). (E) Number of spontaneous lung metastases. Each value corresponds to the median and range of a representative experiment of three independent assays, *p < 0.05 respect to non-treated mice.

cytotoxic activity against human breast cancer cell lines with different expression of ER, PR and Her2/NEU. In the present study, we investigated the effect of T2, the most potent N^4-TSC, on metastasis *in vitro* and in vivo.

Our first results confirmed that T2 had cytotoxic activity on TNBC, since its effects on HCC70, LM38-LP, and 4T1 TNBC cell lines were similar to those found in our previous study [14]. Moreover, the cytotoxic effect of T2 on 4T1 cells was as potent as that observed for Cisplatin and Paclitaxel, chemotherapy agents currently used in first-line therapy for TNBC at present. Next, *in vitro* 4T1 studies suggested that T2 cytotoxic effect was reflected in an increase in apoptosis via caspase-3 activation and a decrease in its clonogenic capacity.

Our next objective was to study whether this N^4-TSC was also able to modulate the remarkable capacity of advanced TNBCs to metastasize, therefore we selected the 4T1 model for the following experiments, for its capacity to grow and disseminate in syngeneic mice and to progress quite similarly to human late-stage breast cancer.

Cell migration and invasion are critical phenomena in cancer cells metastatic dissemination. These processes require degradation of the connective tissue associated with the vascular basal membrane (BM) and interstitial connective tissue [30, 31]. Therefore, invasion through a BM is a crucial step in metastasis [32]. By wound healing and invasion transwell assays, the present study demonstrated that T2 significantly inhibited the migration capacity and invasiveness of 4T1 breast cancer cells in a dose-dependent manner.

Prior to cell invasion through basement membrane barriers, proteolytic degradation is crucial. Several classes of extracellular matrix (ECM)-degrading enzymes are responsible *for* BM and ECM degradation. MMPs are one important class of structurally related ECM-degrading enzymes [33] that are highly regulated and capable of cleaving most of the components of ECM. Consequently, MMPs have been involved as possible links between invasion and metastasis in several tumor models [34, 35, 36, 37]. By zymography assay, we found that T2 inhibited MMP-9 gelatinase activity in 4T1 cells.

Cell motility and consequently metastasis ability are critically dependent on tightly controlled remodeling of actin cytoskeleton. In agreement, our results showed that T2 induced an actin cortical disposition suggesting the change to a more differentiated epithelial phenotype. Further analyses revealed that T2 also increased E-cadherin expression while it reduced αSMA, supporting the hypothesis that T2 treatment may be driving 4T1 cells to a mesenchymal-epithelial transition (MET). We expect that ongoing studies on intermediates such us ZEB1 and Twist will confirm T2 involvement in this process.

CSCs comprise a minor sub-population of almost quiescent cells in the tumor that have the ability to self-renew and differentiate into non-stem daughter cells which would be part of the tumor [38, 39, 40]. Fast proliferating cells are the principal targets of chemotherapy and radiotherapy. Since CSCs remain in the quiescent stage of the cell cycle most of the time [41, 42], they can avoid the damage caused by chemotherapeutic drugs, unlike the rapidly dividing cells, so CSCs survive and then raise recurrent tumors, frequently at metastatic sites [43]. Consequently, drugs with deleterious effects against CSCs should inhibit tumor growth, metastasis, recurrence, and drug resistance. In this study, we demonstrated that T2, a supposed iron chelator, reduced the number of CSCs present in 4T1 cell line and that it also showed a direct cytotoxic effect on CSC mammospheres derived from 4T1 cells. In 2006, Shackleton *et al.* identified a subpopulation of mammary cells, classified as Lin- (negative for endothelial marker CD31 and hematopoietic markers CD45 and TER119), CD29high (β-1 integrin) and CD24+ (a heat-stable antigen expressed on human breast tumors), from which a single cell could differentiate into complex alveolar-like structures that produced milk protein, demonstrating the ability of these cells to reconstitute a complete mammary gland [44]. Therefore, we also evaluated $Lin^-/CD29^h/CD24^+$ cells after T2 treatment and found that T2 reduced this population in 4T1 cell line. Gene expression is also a major consideration when investigating CSCs, with Oct4 (octamer-binding transcription factor 4), Sox2 (sex determining region Y-box 2), and homeobox protein Nanog being recognized as master transcription factors (TFs) controlling pluripotency [45]. Thus, we further studied pluripotency genes expression detecting a lower level in 4T1 cells, after T2 treatment. These results agree with Ninomiya et al [46], who demonstrated that iron

appears to be crucial for the proliferation and maintenance of stemness of CSCs.

Taking into account all the effects shown *in vitro* by T2 on metastasis-related properties, we developed an experimental metastasis assay *in vivo* with 4T1 cells. In accordance, our results showed that T2 *ex-vivo* pre-treatment of 4T1 cells significantly reduced the number of lung metastatic nodules developed 21 days after iv inoculation.

Considering that metastasis is a complex process that demands the modulation of both metastasis-promoting and metastasis suppressor genes, and since NDRG-1 (N-myc downregulated gene 1) is a potential molecular target for cancer therapy regulated by novel thiosemicarbazones [23, 47], we analyzed its modulation after T2 treatment in the same cells. At mRNA level, we observed that T2 did not induce any variation in NDRG-1 expression. However, T2 significantly increased its expression in a dose-dependent manner at protein level, indicating that T2 treatment somehow modulated the translational process. Future studies including protein synthesis inhibition by protein interactions and miRNAs must be done to explore and determine which is the mechanism responsible of this translation modulation.

Finally, further *in vivo* experiments demonstrated that the intraperitoneal administration of T2 reduced the growth of 4T1 tumor without any acute or chronic toxicity observed at the assayed doses. Macroscopic and microscopic observations also showed that T2 reduced in vivo tumor invasiveness. Considering that distant metastasis is the major cause of death in TNBC, we also investigated T2 effect on 4T1 spontaneous metastatic capacity and we found that this N^4-TSC significantly reduced the metastasic nodules in T2-treated mice lungs. This anti-metastasic action of T2 could represent an important advantage over first line chemotherapeutics such as paclitaxel, which has shown to elicits a proinflammatory effect dependent on Toll-like receptors (TLRs) signaling that results in cancer treatment failure, tumor resistance or even induction of the lymph node and pulmonary metastasis of breast cancer [28, 29].

In conclusion, new drug therapies able to overcome existing problems of drug resistance, recurrence and metastasis are urgently required for advanced TNBC. We have been recently exploring the activity of a group of Fe chelators as potential cancer treatment. The best performing chelator, T2, showed *in vitro* pronounced cytotoxic activity against a panel of triple negative breast cancer cell lines including 4T1, LM38-LP and HCC70 cells. Besides, this TSC notably down-modulated 4T1 metastatic-associated properties. Intraperitoneal T2 administration in BALB/c mice showed a remarkable growth inhibition of the syngeneic 4T1 late-stage tumor without evident toxic effects in the host. It was also demonstrated that this N^4-TSC significantly reduced *in vivo* 4T1 tumor invasiveness and metastasis. Finally, our findings highlight T2 as a promising class of compound for further studies concerning new anticancer therapies.

Declarations

Author contribution statement

M. Callero: Conceived and designed the experiments; Performed the experiments; Analyzed and interpreted the data; Wrote the paper.

A. Sólimo: Performed the experiments; Analyzed and interpreted the data.

M. Santacruz, S. Vanzulli, O. Coggiola, L. Filkiensztein: Contributed reagents, materials, analysis tools or data.

E. de Kier Joffé: Contributed reagents, materials, analysis tools or data; Wrote the paper.

Funding statement

This work was supported by Fundación Florencio Fiorini and Universidad de Buenos Aires. A. Sólimo and M. Santacruz were supported by Consejo Nacional de Investigaciones Científicas y Técnicas.

Competing interest statement

The authors declare no conflict of interest.

Additional information

Supplementary content related to this article has been published online at https://doi.org/10.1016/j.heliyon.2020.e05161.

References

[1] F. Bray, J. Ferlay, I. Soerjomataram, R.L. Siegel, L.A. Torre, A. Jemal, Global cancer statistics 2018: GLOBOCAN estimates of incidence and mortality worldwide for 36 cancers in 185 countries, CA, Cancer J. Clin. 68 (2018) 394–424.

[2] C.W.S. Tong, M. Wu, W.C.S. Cho, K.K.W. To, Recent advances in the treatment of breast cancer, Front. Oncol. 8 (2018) 227.

[3] A.C. Wolff, M.E.H. Hammond, D.G. Hicks, M. Dowsett, L.M. McShane, K.H. Allison, D.C. Allred, J.M.S. Bartlett, M. Bilous, P. Fitzgibbons, W. Hanna, R.B. Jenkins, P.B. Mangu, S. Paik, E.A. Perez, M.F. Press, P.A. Spears, G.H. Vance, G. Viale, D.F. Hayes, American society of clinical Oncology, college of American pathologists, recommendations for human epidermal growth factor receptor 2 testing in breast cancer: American society of clinical oncology/college of American pathologists clinical practice guideline update, Arch. Pathol. Lab Med. 138 (2014) 241–256.

[4] M.E.H. Hammond, D.F. Hayes, A.C. Wolff, P.B. Mangu, S. Temin, American society of clinical oncology/college of American pathologists guideline recommendations for immunohistochemical testing of estrogen and Progesterone receptors in breast cancer, J. Oncol. Pract. 6 (2010) 195–197.

[5] R. Haque, S.A. Ahmed, G. Inzhakova, J. Shi, C. Avila, J. Polikoff, L. Bernstein, S.M. Enger, M.F. Press, Impact of breast cancer subtypes and treatment on survival: an analysis spanning two decades, Cancer Epidemiol. Biomark. Prev. 21 (2012) 1848–1855.

[6] C. Denkert, C. Liedtke, A. Tutt, G. von Minckwitz, Molecular alterations in triple-negative breast cancer—the road to new treatment strategies, Lancet 389 (2017) 2430–2442.

[7] H. Yao, G. He, S. Yan, C. Chen, L. Song, T.J. Rosol, X. Deng, Triple-negative breast cancer: is there a treatment on the horizon? Oncotarget 8 (2017) 1913–1924.

[8] P. Khosravi-Shahi, L. Cabezón-Gutiérrez, S. Custodio-Cabello, Metastatic triple negative breast cancer: optimizing treatment options, new and emerging targeted therapies., Asia, Pac. J. Clin. Oncol. 14 (2018) 32–39.

[9] H. Yagata, Y. Kajiura, H. Yamauchi, Current strategy for triple-negative breast cancer: appropriate combination of surgery, radiation, and chemotherapy, Breast Cancer 18 (2011) 165–173.

[10] Z.-L. Guo, D.R. Richardson, D.S. Kalinowski, Z. Kovacevic, K.C. Tan-Un, G.C.-F. Chan, The novel thiosemicarbazone, di-2-pyridylketone 4-cyclohexyl-4-methyl-3-thiosemicarbazone (DpC), inhibits neuroblastoma growth in vitro and in vivo via multiple mechanisms, J. Hematol. Oncol. 9 (2016) 98.

[11] C. Stefani, P.J. Jansson, E. Gutierrez, P.V. Bernhardt, D.R. Richardson, D.S. Kalinowski, Alkyl substituted 2′-benzoylpyridine thiosemicarbazone chelators with potent and selective anti-neoplastic activity: novel ligands that limit methemoglobin formation, J. Med. Chem. 56 (2013) 357–370.

[12] G.Y.L. Lui, P. Obeidy, S.J. Ford, C. Tselepis, D.M. Sharp, P.J. Jansson, D.S. Kalinowski, Z. Kovacevic, D.B. Lovejoy, D.R. Richardson, The iron chelator, deferasirox, as a novel strategy for cancer treatment: oral activity against human lung tumor xenografts and molecular mechanism of action, Mol. Pharmacol. 83 (2013) 179–190.

[13] P.J. Jansson, T. Yamagishi, A. Arvind, N. Seebacher, E. Gutierrez, A. Stacy, S. Maleki, D. Sharp, S. Sahni, D.R. Richardson, Di-2-pyridylketone 4,4-dimethyl-3-thiosemicarbazone (Dp44mT) overcomes multidrug resistance by a novel mechanism involving the hijacking of lysosomal P-glycoprotein (Pgp), J. Biol. Chem. 290 (2015) 9588–9603.

[14] A. Sólimo, M. Soraires Santacruz, A. Loaiza Perez, E. Bal de Kier Joffé, L. Finkielsztein, M. Callero, N^4 -aryl substituted thiosemicarbazones derived from 1-indanones as potential anti-tumor agents for breast cancer treatment, J. Cell. Physiol. (2017).

[15] L. Chen, T.G. Huang, M. Meseck, J. Mandeli, J. Fallon, S.L.C. Woo, Rejection of metastatic 4T1 breast cancer by attenuation of treg cells in combination with immune stimulation, Mol. Ther. 15 (2007) 2194–2202.

[16] K. Tao, M. Fang, J. Alroy, G.G. Gary, Imagable 4T1 model for the study of late stage breast cancer, BMC Canc. 8 (2008).

[17] V. Bumaschny, A. Urtreger, M. Diament, M. Krasnapolski, G. Fiszman, S. Klein, E.B. de K. Joffé, Malignant myoepithelial cells are associated with the differentiated papillary structure and metastatic ability of a syngeneic murine mammary adenocarcinoma model, Breast Cancer Res. 6 (2004) R116–R129.

[18] A.H. Cory, T.C. Owen, J.A. Barltrop, J.G. Cory, Use of an aqueous soluble tetrazolium/formazan assay for cell growth assays in culture, Canc. Commun. 3 (1991) 207–212. http://www.ncbi.nlm.nih.gov/pubmed/1867954. (Accessed 15 November 2017).

[19] R.B. Tajhya, R.S. Patel, C. Beeton, Detection of matrix metalloproteinases by zymography, in: Methods Mol. Biol., Humana Press Inc., 2017, pp. 231–244.

[20] C.S. Hughes, L.M. Postovit, G.A. Lajoie, Matrigel: a complex protein mixture required for optimal growth of cell culture, Proteomics 10 (2010) 1886–1890.

[21] M. McKinney, M. Robbins, Chronic atropine administration up-regulates rat cortical

muscarinic m1 receptor mRNA molecules: assessment with the RT/PCR, Mol. Brain Res. 12 (1992) 39–45.
[22] M.M. Bradford, A rapid and sensitive method for the quantitation of microgram quantities of protein utilizing the principle of protein-dye binding, Anal. Biochem. 72 (1976) 248–254. http://www.ncbi.nlm.nih.gov/pubmed/942051. (Accessed 9 February 2017).
[23] Z. Kovacevic, S. Chikhani, D.B. Lovejoy, D.R. Richardson, Novel thiosemicarbazone iron chelators induce up-regulation and phosphorylation of the metastasis suppressor N-myc down-stream regulated gene 1: a new strategy for the treatment of pancreatic cancer, Mol. Pharmacol. 80 (2011) 598–609.
[24] S. Bandyopadhyay, S.K. Pai, S.C. Gross, S. Hirota, S. Hosobe, K. Miura, K. Saito, T. Commes, S. Hayashi, M. Watabe, K. Watabe, The Drg-1 gene suppresses tumor metastasis in prostate cancer, Canc. Res. 63 (2003) 1731–1736. http://www.ncbi.nlm.nih.gov/entrez/query.fcgi?cmd=Retrieve&db=PubMed&dopt=Citation&list_uids=12702552.
[25] R.J. Guan, H.L. Ford, Y. Fu, Y. Li, L.M. Shaw, A.B. Pardee, Drg-1 as a differentiation-related, putative metastatic suppressor gene in human colon cancer, Canc. Res. 60 (2000) 749–755. http://www.ncbi.nlm.nih.gov/pubmed/10676663. (Accessed 7 December 2018).
[26] W. Liu, F. Xing, M. Iiizumi-Gairani, H. Okuda, M. Watabe, S.K. Pai, P.R. Pandey, S. Hirota, A. Kobayashi, Y.-Y. Mo, K. Fukuda, Y. Li, K. Watabe, N-myc downstream regulated gene 1 modulates Wnt-β-catenin signalling and pleiotropically suppresses metastasis, EMBO Mol. Med. 4 (2) (2012) 93–108, https://doi.org/10.1002/emmm.201100190.
[27] M.A. Soares, J.A. Lessa, I.C. Mendes, J.G. Da Silva, R.G. Dos Santos, L.B. Salum, H. Daghestani, A.D. Andricopulo, B.W. Day, A. Vogt, J.L. Pesquero, W.R. Rocha, H. Beraldo, N^4-Phenyl-substituted 2-acetylpyridine thiosemicarbazones: cytotoxicity against human tumor cells, structure-activity relationship studies and investigation on the mechanism of action, Bioorg. Med. Chem. 20 (2012) 3396–3409.
[28] D.R. Richardson, P.C. Sharpe, D.B. Lovejoy, D. Senaratne, D.S. Kalinowski, M. Islam, P.V. Bernhardt, Dipyridyl thiosemicarbazone chelators with potent and selective antitumor activity form iron complexes with redox activity, J. Med. Chem. 49 (2006) 6510–6521.
[29] Y. Yu, D.S. Kalinowski, Z. Kovacevic, A.R. Siafakas, P.J. Jansson, C. Stefani, D.B. Lovejoy, P.C. Sharpe, P.V. Bernhardt, D.R. Richardson, Thiosemicarbazones from the old to new: iron chelators that are more than just ribonucleotide reductase inhibitors, J. Med. Chem. 52 (2009) 5271–5294.
[30] P. Pandya, J.L. Orgaz, V. Sanz-Moreno, Modes of invasion during tumour dissemination, Mol. Oncol. 11 (2017) 5–27.
[31] M.F. Leber, T. Efferth, Molecular principles of cancer invasion and metastasis (review), Int. J. Oncol. 34 (2009) 881–895. http://www.ncbi.nlm.nih.gov/pubmed/19287945. (Accessed 10 December 2018).
[32] P. Jiang, A. Enomoto, M. Takahashi, Cell biology of the movement of breast cancer cells: intracellular signalling and the actin cytoskeleton, Canc. Lett. 284 (2009) 122–130.
[33] O.R.F. Mook, W.M. Frederiks, C.J.F. Van Noorden, The role of gelatinases in colorectal cancer progression and metastasis, Biochim. Biophys. Acta Rev. Canc 1705 (2004) 69–89.
[34] P. Foidart, C. Yip, J. Radermacher, M. Lienard, S. Blacher, L. Montero-Ruiz, E. Maquoi, E. Montaudon, S. Chateau-Joubert, J. Collignon, M. Coibion, V. Jossa, E. Marangoni, A. Noel, N.E. Sounni, G. Jerusalem, Expression of MT4-MMP, EGFR and RB in triple negative breast cancer strongly sensitizes tumors to erlotinib and palbociclib combination therapy, Clin. Canc. Res. (2018).
[35] B. Gru nwald, J. Vandooren, M. Gerg, K. Ahomaa, A. Hunger, S. Berchtold, S. Akbareian, S. Schaten, P. Knolle, D.R. Edwards, G. Opdenakker, A. Kru ger, Systemic ablation of MMP-9 triggers invasive growth and metastasis of pancreatic cancer via deregulation of IL6 expression in the bone marrow, Mol. Canc. Res. 14 (2016) 1147–1158.
[36] Y. Li, B. Sun, X. Zhao, X. Wang, D. Zhang, Q. Gu, T. Liu, MMP-2 and MMP-13 affect vasculogenic mimicry formation in large cell lung cancer, J. Cell Mol. Med. 21 (2017) 3741–3751.
[37] W. Zhong, Z. Han, H. He, X. Bi, Q. Dai, G. Zhu, Y. Ye, Y. Liang, W. Qin, Z. Zhang, G. Zeng, Z. Chen, CD147, MMP-1, MMP-2 and MMP-9 protein expression as significant prognostic factors in human prostate cancer, Oncology 75 (2008) 230–236.
[38] F. Saeg, M. Anbalagan, Breast cancer stem cells and the challenges of eradication: a review of novel therapies, Stem Cell Invest. 5 (2018) 39, 39.
[39] N.Y. Frank, T. Schatton, M.H. Frank, The therapeutic promise of the cancer stem cell concept, J. Clin. Invest. 120 (2010) 41–50.
[40] P.B. Gupta, C.L. Chaffer, R.A. Weinberg, Cancer stem cells: mirage or reality? Nat. Med. 15 (2009) 1010–1012.
[41] S. Pece, D. Tosoni, S. Confalonieri, G. Mazzarol, M. Vecchi, S. Ronzoni, L. Bernard, G. Viale, P.G. Pelicci, P.P. Di Fiore, Biological and molecular heterogeneity of breast cancers correlates with their cancer stem cell content, Cell 140 (2010) 62–73.
[42] A. Wilson, E. Laurenti, G. Oser, R.C. van der Wath, W. Blanco-Bose, M. Jaworski, S. Offner, C.F. Dunant, L. Eshkind, E. Bockamp, P. Lió, H.R. MacDonald, A. Trumpp, Hematopoietic stem cells reversibly switch from dormancy to self-renewal during homeostasis and repair, Cell 135 (2008) 1118–1129.
[43] J. Zhao, Cancer stem cells and chemoresistance: the smartest survives the raid, Pharmacol. Ther. 160 (2016) 145–158.
[44] M. Shackleton, F. Vaillant, K.J. Simpson, J. Stingl, G.K. Smyth, M.-L. Asselin-Labat, L. Wu, G.J. Lindeman, J.E. Visvader, Generation of a functional mammary gland from a single stem cell, Nature 439 (2006) 84–88.
[45] L.A. Boyer, T.I. Lee, M.F. Cole, S.E. Johnstone, S.S. Levine, J.P. Zucker, M.G. Guenther, R.M. Kumar, H.L. Murray, R.G. Jenner, D.K. Gifford, D.A. Melton, R. Jaenisch, R.A. Young, Core transcriptional regulatory circuitry in human embryonic stem cells, Cell 122 (2005) 947–956.
[46] T. Ninomiya, T. Ohara, K. Noma, Y. Katsura, R. Katsube, H. Kashima, T. Kato, Y. Tomono, H. Tazawa, S. Kagawa, Y. Shirakawa, F. Kimura, L. Chen, T. Kasai, M. Seno, A. Matsukawa, T. Fujiwara, Iron depletion is a novel therapeutic strategy to target cancer stem cells, Oncotarget 8 (2017) 98405–98416.
[47] Z. Chen, D. Zhang, F. Yue, M. Zheng, Z. Kovacevic, D.R. Richardson, The iron chelators Dp44mT and DFO inhibit TGF-β-induced epithelial-mesenchymal transition via up-regulation of N-Myc downstream-regulated gene 1 (NDRG1), J. Biol. Chem. 287 (2012) 17016–17028.